Expert Systems with Applications 37 (2010) 1050–1055

Contents lists available at ScienceDirect

Expert Systems with Applications

journal homepage: www.elsevier.com/locate/eswa

An intelligent maximum power point tracking method based on extension theory for PV systems

Kuei-Hsiang Chao *, Ching-Ju Li

Department of Electrical Engineering, National Chin-Yi University of Technology, Taiwan

ARTICLE INFO

Keywords:
Intelligent maximum power point tracking (MPPT)
Photovoltaic (PV) system
Perturbation and observation (P&O) method
Incremental conductance (INC) method
Extension theory

ABSTRACT

The purpose of this paper is to propose a novel maximum power point tracking (MPPT) technique to fully utilize photovoltaic (PV) array output power that depends on solar insolation and ambient temperature. The proposed intelligent MPPT algorithm based on extension theory can automatically adjust the step size to track the PV array maximum power point (MPP). Compared with the conventional fixed step size perturbation and observation (P&O) and incremental conductance (INC) methods, the presented approach is able to effectively improve the dynamic response and steady-state performance of the PV systems simultaneously. Theoretical analysis and the design principle of the proposed method are described in detail. Some simulations are performed to demonstrate the effectiveness of the proposed extension MPPT method.

1. Introduction

Recently, many techniques have been proposed for tracking the maximum power point of PV arrays (Desai & Patel, 2007; Esram & Chapman, 2007; Femia, Granozio, Petrone, Spagnuolo, & Vitelli, 2007; Godoy Simoes & Franceschetti, 1999; Koutroulis, Kalaitzakis, & Voulgaris, 2001; Liu, Duan, Liu, & Kang, 2008; Masoum, Dehbonei, & Fuchs, 2002; Sera, Kerekes, Teodorescu, & Blaabjerg, 2006; Wu, Zhao, & Liu, 2007). The voltage and current based photovoltaic generator methods (Masoum et al., 2002) offer a simple and low-priced way to gain maximum power. Nevertheless, they require periodical disconnection or short-circuiting of the PV modules to measure the open-circuit voltage or short-circuit current for reference, resulting in more power loss when scanning the entire control range. The perturbation and observation (P&O) method (Esram & Chapman, 2007; Femia et al., 2007; Sera et al., 2006) is widely applied in the MPPT controller due to its simplicity and easy implementation, but its accuracy in steady-state is low because the perturbation process would make the operation point of the PV arrays oscillate around the MPP. Therefore, the power loss may increase. Further, when the insolation changes rapidly, the P&O method probably fails to track MPP. The incremental conductance (INC) method (Desai & Patel, 2007; Koutroulis et al., 2001; Wu et al., 2007), which is based on the fact the slope of the PV array power versus voltage curve is zero at the MPP, has been proposed to improve the tracking accuracy and dynamic performance under rapidly varying conditions. The steady-state oscillations would be eliminated in theory since the derivative of the power with respect to the voltage vanishes at MPP. However, the null value of the slope of the PV array power versus voltage curve seldom occurs because of the resolution of digital implementation. The INC MPPT algorithm usually uses a fixed iteration step size, which is determined by the accuracy and tracking speed requirement. Thus, the corresponding design should satisfactorily address the tradeoff between the dynamics and steady state oscillation. To solve these problems, a modified INC MPPT with variable step size and constant voltage tracking (CVT) at the start process (Liu et al., 2008) has been proposed to tune the step size automatically according to the inherent PV array characteristics. However, the high complexity of the method requires high sampling accuracy and fast control speed, which might have resulted in a high cost system. Also, the system stability problem would occur once the control unit switches from CVT to INC MPPT mode or the starting point is not selected properly. The intelligent fuzzy, sliding-mode and neural network methods (Godoy Simoes & Franceschetti, 1999; Khaehintung & Sirisuk, 2007; Kim, Kim, & Youn, 2006; Kottas, Boutalis, & Karlis, 2006; Veerachary, Senjyu, & Uezato, 2003; Wu, Chang, & Chen, 2000) focusing on the nonlinear characteristics of PV array provide a good alternative for MPPT control. Since the output characteristics of the PV array should be well understood to create the MPPT control rules and the computation time of these algorithms are highly complex, the versatility of these methods is limited.

In considering the aforementioned drawbacks and then to fulfill the requirements of dynamic response and steady-state performance of an MPPT control for PV arrays, an intelligent control

* Corresponding author. Tel.: +886 4 2392 4505x7272; fax: +886 4 2392 2156.
E-mail addresses: chaokh@ncut.edu.tw, chaokh0706@yahoo.com.tw (K.-H. Chao).

0957-4174/$ - see front matter © 2009 Elsevier Ltd. All rights reserved.
doi:10.1016/j.eswa.2009.06.068

Table 1
Three different sorts of mathematical sets.

Compared item	Cantor set	Fuzzy set	Extension set
Research objects	Data variables	Linguistic variables	Contradictory problems
Model	Mathematics model	Fuzzy mathematics model	Matter-element model
Descriptive function	Transfer function	Membership function	Correlation function
Descriptive property	Precision	Ambiguity	Extension
Range of set	$C_A(x) \in \{0,1\}$	$\mu_A(x) \in [0,1]$	$K_A(x) \in (-\infty,\infty)$

algorithm based on the P&O method with extension theory (Cai, 1983) is proposed in this paper. The proposed MPPT method can adjust the step size adaptively in response to varying solar insolation and ambient temperature. Less constructed data utilized means no learning procedures and a high convergence rate are needed. These are the good features of the proposed algorithm for improving the dynamic response and steady-state performance of an MPPT control method.

2. Summary of extension theory

In the Cantor set, an element either belongs to or does not belong to a set. Therefore, the range of the Cantor set is {0,1} can be used to solve a two-valued problem. In contrast to the standard set, the fuzzy set allows for describing concepts in which the boundary is not explicit. It concerns not only whether an element belongs to the set but also to what degree it belongs. The range of a fuzzy set is [0,1]. However, the extension set extends the fuzzy set from [0,1] to $(-\infty,\infty)$. As a result, it allows us to define a set including any data in the domain (Cai, 1983). Extension theory tries to solve the incompatibility or contradiction problems by transformation of the matter-element (Cai, 1983). The matter-element theory includes extension theory of the matter-element and the transformation theory of the matter-element. Extension mathematics, based on the extension set, is the quantitative tool for solving problems. Comparisons of the standard sets, fuzzy sets and extension sets are shown in Table 1.

2.1. The matter-element theory

In extension theory, a matter-element (R) contains three fundamental elements: matter name (N), matter characteristics (C) and values of matter characteristics (V). The matter-element can be described as follows:

$$R = (N, C, V) \tag{1}$$

where C is a matter characteristic or a characteristic vector, ex: $C = [c_1, c_2, \ldots, c_n]$, and V the same as C is a value or a vector, ex: $V = [v_1, v_2, \ldots, v_n]$.

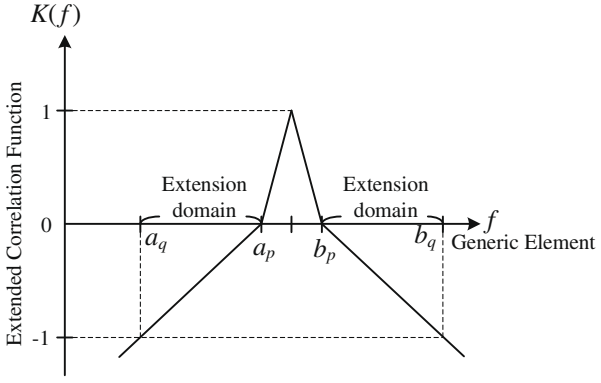

Fig. 1. The extension correlation function.

2.2. Definition of classical and neighborhood domains

If we set $F_0 = \langle a_p, b_p \rangle$, $F = \langle a_q, b_q \rangle$, f is a point in F, then a matter-element R_0 of F_0 can be described as follows:

$$R_0 = (F_0, C, V_p) = \begin{bmatrix} F_0, & c_1, & V_{p1} \\ & c_2, & V_{p2} \\ & \vdots & \vdots \\ & c_n, & V_{pn} \end{bmatrix} = \begin{bmatrix} F_0, & c_1, & \langle a_{p1}, b_{p1} \rangle \\ & c_2, & \langle a_{p2}, b_{p2} \rangle \\ & \vdots & \vdots \\ & c_n, & \langle a_{pn}, b_{pn} \rangle \end{bmatrix} \tag{2}$$

where C are the characteristics of F_0, and V_p are the ranges of C called the classical domains. Similarly, a matter-element R_F of F can be also described as follows:

$$R_F = (F, C, V_q) = \begin{bmatrix} F, & c_1, & V_{q1} \\ & c_2, & V_{q2} \\ & \vdots & \vdots \\ & c_n, & V_{qn} \end{bmatrix} = \begin{bmatrix} F, & c_1, & \langle a_{q1}, b_{q1} \rangle \\ & c_2, & \langle a_{q2}, b_{q2} \rangle \\ & \vdots & \vdots \\ & c_n, & \langle a_{qn}, b_{qn} \rangle \end{bmatrix} \tag{3}$$

Also, V_q are the ranges of C called the neighborhood domains.

2.3. Definition of correlation function

If $F_0 \in F$, then the extended correlation function $K(f)$ can be defined as follows:

$$K(f) = \frac{\rho(f, F_0)}{D(f, F_0, F)} \tag{4}$$

If one wants to set $K(f) \leqslant 1$, then

$$\rho(f, F_0) = \left| f - \frac{a_p + b_p}{2} \right| - \frac{b_p - a_p}{2} \tag{5}$$

$$D(f, F_0, F) = \begin{cases} \rho(f, F) - \rho(f, F_0) & \text{for } f \notin F_0 \\ -\frac{|(a_p - b_p)|}{2} & \text{for } f \in F_0 \end{cases} \tag{6}$$

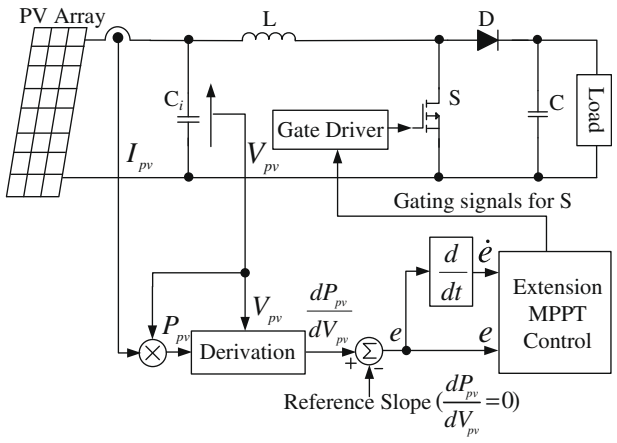

Fig. 2. The proposed extension MPPT scheme.

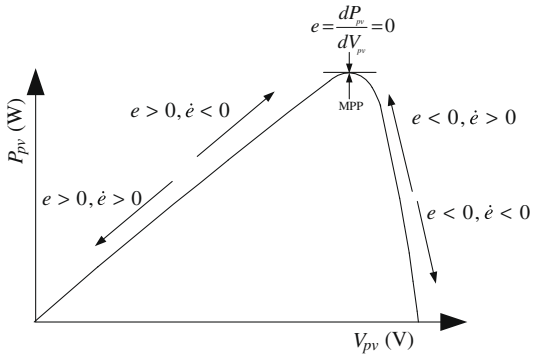

Fig. 3. The $P-V$ curve slope e error and error change of PV arrays.

where

$$\rho(f,F)=\left|f-\frac{a_q+b_q}{2}\right|-\frac{b_q-a_q}{2} \tag{7}$$

The correlation function can be used to calculate the membership grade between f and F_0. The extended correlation function is shown in Fig. 1. When $K(f)\geqslant 0$, this indicates the degrees to which f belongs to F_0. When $K(f)<0$ it describes the degree to which f does not belong to F_0. When $-1<K(f)<0$, it is called the extension domain, which means the element f still has a probability of becoming part of the set if the conditions change.

3. The extension MPPT controller

3.1. The proposed MPPT scheme

A simple MPPT PV system shown in Fig. 2 is developed to test the effectiveness of the proposed method. A boost converter is used as the power interface between the PV array and the load to achieve maximum power. The output voltage V_o of the boost converter can be expressed as (Hart, 1997).

$$V_o=\frac{V_s}{1-D} \tag{8}$$

where D is the duty cycle of the converter. It can be seen the input DC voltage V_s can be shifted to a high level. This power converter is

Table 3
The classical domains of categories.

Category	Classical domain
1	$R_1=\begin{bmatrix}F_0 & c_1 & \langle 0,15\rangle\\ & c_2 & \langle -100,0\rangle\end{bmatrix}$
2	$R_2=\begin{bmatrix}F_0 & c_1 & \langle 15,20\rangle\\ & c_2 & \langle -100,0\rangle\end{bmatrix}$
3	$R_3=\begin{bmatrix}F_0 & c_1 & \langle 20,50\rangle\\ & c_2 & \langle -100,0\rangle\end{bmatrix}$
4	$R_4=\begin{bmatrix}F_0 & c_1 & \langle 0,15\rangle\\ & c_2 & \langle 0,100\rangle\end{bmatrix}$
5	$R_5=\begin{bmatrix}F_0 & c_1 & \langle 15,20\rangle\\ & c_2 & \langle 0,100\rangle\end{bmatrix}$
6	$R_6=\begin{bmatrix}F_0 & c_1 & \langle 20,50\rangle\\ & c_2 & \langle 0,100\rangle\end{bmatrix}$
7	$R_7=\begin{bmatrix}F_0 & c_1 & \langle -90,0\rangle\\ & c_2 & \langle -100,0\rangle\end{bmatrix}$
8	$R_8=\begin{bmatrix}F_0 & c_1 & \langle -230,-90\rangle\\ & c_2 & \langle -100,0\rangle\end{bmatrix}$
9	$R_9=\begin{bmatrix}F_0 & c_1 & \langle -350,-90\rangle\\ & c_2 & \langle -100,0\rangle\end{bmatrix}$
10	$R_{10}=\begin{bmatrix}F_0 & c_1 & \langle -90,0\rangle\\ & c_2 & \langle 0,100\rangle\end{bmatrix}$
11	$R_{11}=\begin{bmatrix}F_0 & c_1 & \langle -230,-90\rangle\\ & c_2 & \langle 0,100\rangle\end{bmatrix}$
12	$R_{12}=\begin{bmatrix}F_0 & c_1 & \langle -350,-230\rangle\\ & c_2 & \langle 0,100\rangle\end{bmatrix}$

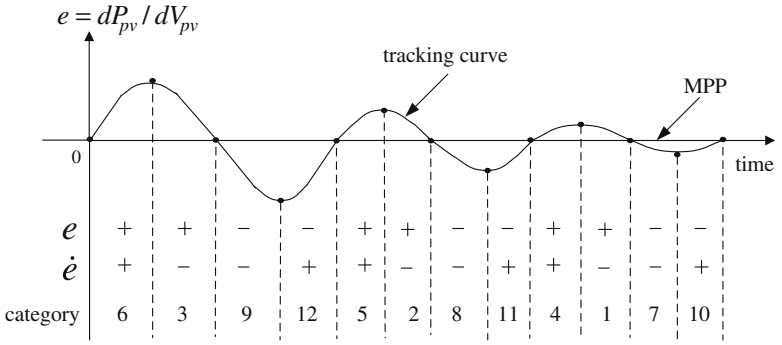

Fig. 4. General dP_{pv}/dV_{pv} reference tracking error dynamic behavior.

Table 2
Quantized slope e error and error change and decision duty cycle.

Category number	Slope error category e	Slope e error change category $\dot{e}$	Duty cycle step size ΔD	Error change polarity
1	$0<e\leqslant 15$	$-100<\dot{e}\leqslant 0$	−0.01	+1
2	$15<e\leqslant 20$	$-100<\dot{e}\leqslant 0$	−0.03	+1
3	$20<e\leqslant 50$	$-100<\dot{e}\leqslant 0$	−0.05	+1
4	$0<e\leqslant 15$	$0<\dot{e}\leqslant 100$	−0.01	−1
5	$15<e\leqslant 20$	$0<\dot{e}\leqslant 100$	−0.03	−1
6	$20<e\leqslant 50$	$0<\dot{e}\leqslant 100$	−0.05	−1
7	$-90<e\leqslant 0$	$-100<\dot{e}\leqslant 0$	0.03	−1
8	$-230<e\leqslant -90$	$-100<\dot{e}\leqslant 0$	0.04	−1
9	$-350<e\leqslant -230$	$-100<\dot{e}\leqslant 0$	0.05	−1
10	$-90<e\leqslant 0$	$0<\dot{e}\leqslant 100$	0.03	+1
11	$-230<e\leqslant -90$	$0<\dot{e}\leqslant 100$	0.04	+1
12	$-350<e\leqslant -230$	$0<\dot{e}\leqslant 100$	0.05	+1

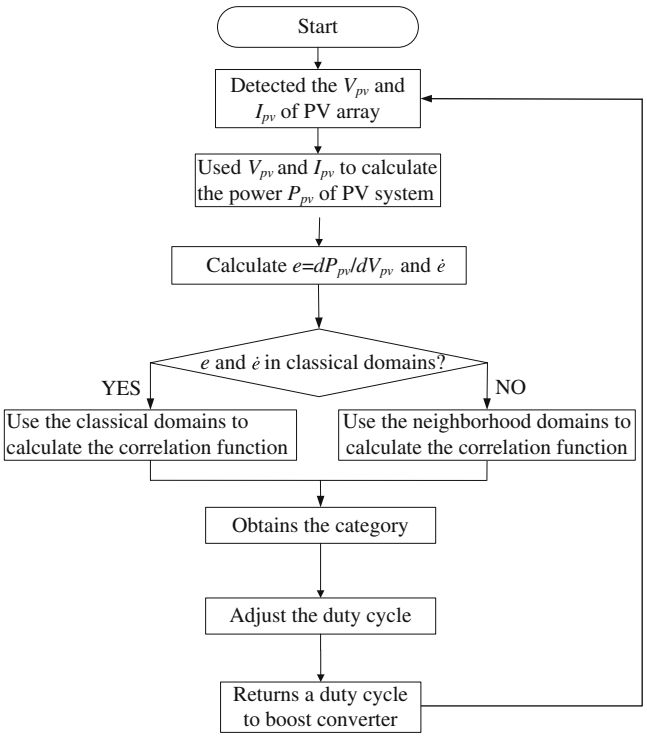

Fig. 5. The flowchart of the extension MPPT algorithm.

suitable for a lower PV output voltage and higher desirable DC link voltage case.

3.2. The extension MPPT method

To let the MPPT method possess adaptive capability, it is proposed the step size of the P&O MPPT method of the PV arrays is adaptively tuned by the extension error tuning scheme, which is driven by a slope error of the PV array power P_{pv} versus voltage V_{pv} and its error change which are defined as $e(k) \triangleq \frac{\Delta}{} \frac{P_{pv}(k)-P_{pv}(k-1)}{V_{pv}(k)-V_{pv}(k-1)} - 0 = \frac{dP_{pv}(k)}{dV_{pv}(k)}$ and $\dot{e}(k) \triangleq \frac{\Delta}{} e(k) - e(k-1)$ with $P_{pv}(k)$ and $V_{pv}(k)$ being the output power and voltage of the PV arrays at kth sampling interval, respectively. The major purpose of this MPPT controller is to let the resulting dP_{pv}/dV_{pv} tracking response closely follow the reference $dP_{pv}/dV_{pv} = 0$, as shown in Fig. 3. Thus, the general model error trajectory can be predicted and plotted in Fig. 4. Based on the experience of the $P - V$ characteristic curve shown in Fig. 3 and incorporating with the extension matter-element, the numbers of quantization levels of the input variables $e(k)$ and $\dot{e}(k)$ are chosen to be 12 categories and listed in Table 2. Based on the experience of the MPP to be controlled and the properties of dynamic signal analyses made in Fig. 4, the linguistic rules of the extension error tuning scheme are decided and listed in the Table 2. The slope error e is equal to zero at MPP of the PV array. When the operation point closes to MPP, slope error e decreases; on the contrary, the value of e will increase. And, the polarity of error change depends on the voltage changing direction, as shown in Fig. 3. According to the range of e and $\dot{e}$, the extension MPPT algorithm can discriminate the category and then determine the duty cycle of the boost converter.

According to the $P - V$ curve statistical records of PV arrays at 200 W/m^2–1000 W/m^2, the value ranges $\langle a_p, b_p \rangle$ of classical regions for each characteristic are assigned by the lower and upper boundary of statistical records as shown in Table 3. In addition, one can set a matter-element model to express the neighborhood domain of every characteristic for describing the possible range of all slope errors and error change. The value range $\langle a_q, b_q \rangle$ of the neighborhood domain could be determined from the maximum and minimum values of every characteristic in the statistical records. For the selected solar insolation range 200 W/m^2–1000 W/m^2, it can be represented as:

$$R_F = (F, C, V_q) = \begin{bmatrix} F & c_1 & \langle -350, 50 \rangle \\ & c_2 & \langle -100, 100 \rangle \end{bmatrix} \tag{9}$$

After establishing the matter-element model based on the extension method, the MPPT can be controlled properly.

The flow chart of the proposed extension MPPT method is shown in Fig. 5, and its process is summarized as below (Chao, Ho, & Wang, 2008):

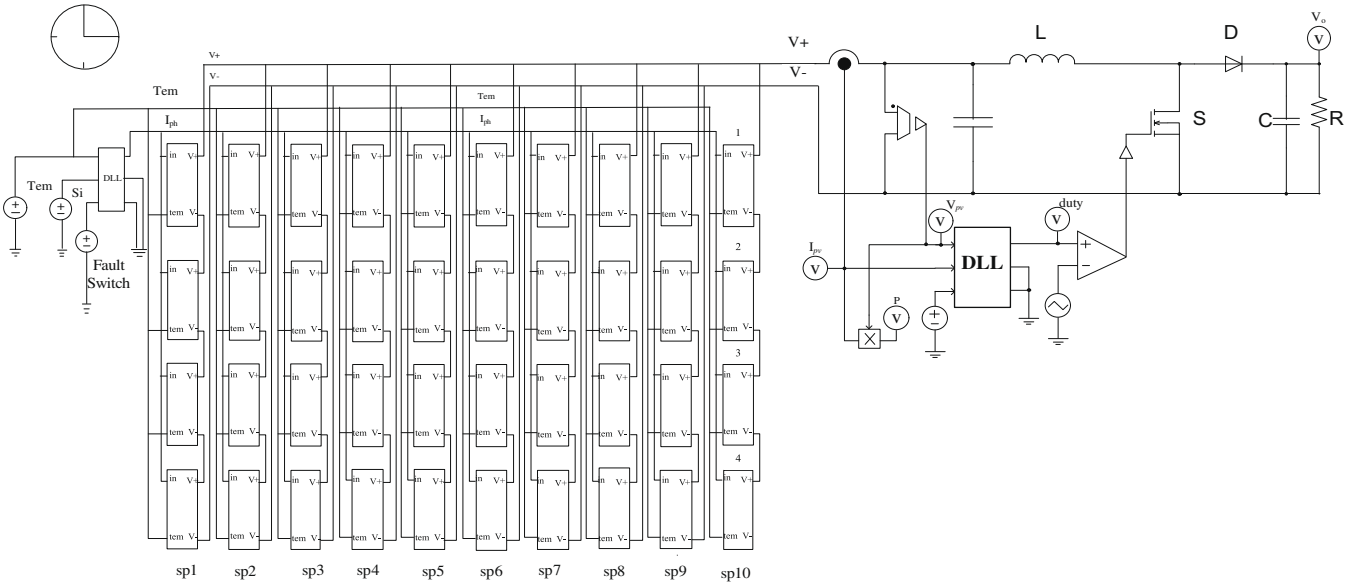

Fig. 6. The 3 kW PV array PSIM model with 4 × 10 series-parallel connection in simulation.

Step 1. Establish the matter-element model of slope error and error changes category, which is performed as follows:

$$R_k = \begin{bmatrix} F_0 & c_1 & V_{p1k} \\ & c_2 & V_{p2k} \end{bmatrix}, \quad k = 1, 2, \ldots, 12 \tag{10}$$

where $V_{pjk} = \langle a_{pjk}, b_{pjk} \rangle$, $j = 1,2$ is the classical domain of every characteristic set.

Step 2. Set the matter-element of the input slope error and error change as (11):

$$R_{new} = \begin{bmatrix} F_{new}, & c_1, & V_{new1} \\ & c_2, & V_{new2} \end{bmatrix} \tag{11}$$

Step 3. Calculate the correlation degrees of the slope errors and error changes with the characteristic of each matter-element by the proposed extended correlation function shown in (4).

Step 4. Assign weights to the matter characteristic such as W_1, W_2 denoting the significance of every characteristic. In this paper, W_1, W_2 are set as $W_1 = 0.85$, $W_2 = 0.15$.

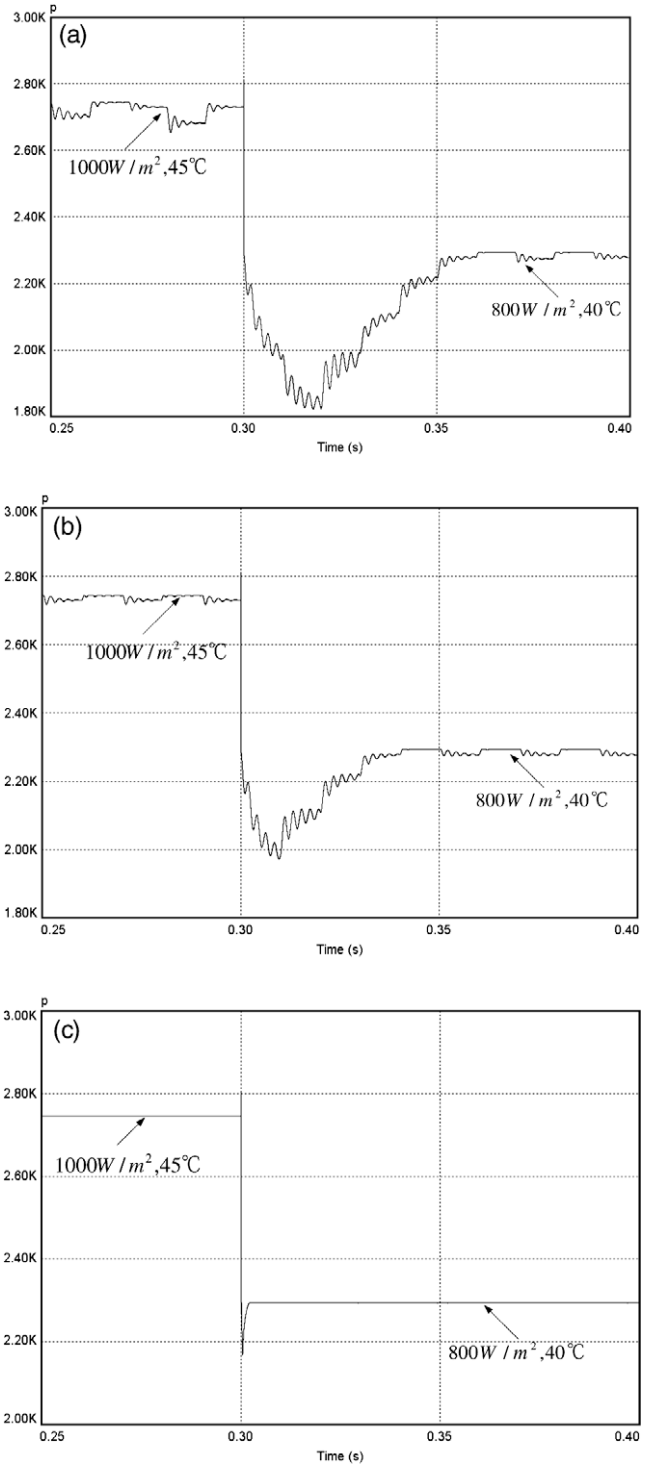

Fig. 7. Simulated dynamic response of PV array output power due to solar insolation step change from 1000 W/m^2 to 800 W/m^2 with (a) P&Q MPPT method; (b) INC MPPT method; (c) the proposed extension MPPT method.

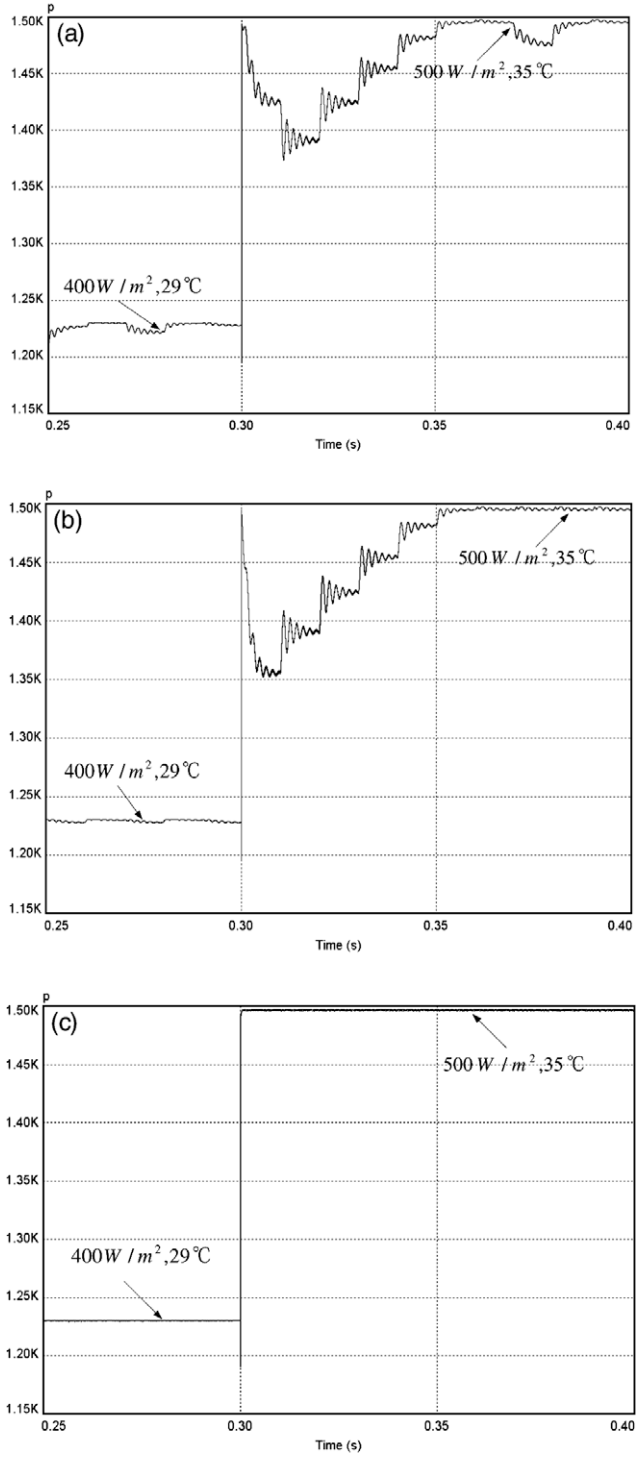

Fig. 8. Simulated dynamic response of PV array output power due to solar insolation step change from 400 W/m^2 to 500 W/m^2 with (a) P&Q MPPT method; (b) INC MPPT method; (c) the proposed extension MPPT method.

Step 5. Calculate the correlation degrees of every category:

$$K(f)_k = \sum_{j=1}^{2} W_j K_{kj}, \quad (k = 1, 2, \ldots, 12) \tag{12}$$

Step 6. Select the maximum value from the normal correlation degrees to recognize the category of the input slope error and error change information and determine the duty cycle step size ΔD of the boost converter and the polarity p of error change $\dot{e}$. To increase the sensitivity and adaptive capability, the new duty cycle D_{new} in the next time period is determined as follows:

$$D_{new} = D_{old} + \Delta D + (\Delta D \times p \times (K(f) - 1)) \tag{13}$$

where D_{old} is the duty cycle of the boost converter in the previous sample period, $K(f)$ is the maximum correlation degrees of the category.

Step 7. Input a new slope error and error change, then return to Step 2, or else end the process.

4. Simulation results

To verify the performance of the proposed extension MPPT algorithm, a circuit-based PSIM model of the PV system shown in Fig. 6 is developed (Chao et al., 2008; Powersim Inc., 2001–2003). SIEMENS SP75 Crystalline Silicon 75W PV module whose specifications can be found in (Siemens Solar Industries, 1998) is used to form a 3 kW PV array model with 4 × 10 series-parallel connection for simulation. The extension MPPT control algorithm is modeled in the external dynamic link library (DLL) block, which is written in C/C++code. The boost converter specifications are chosen as follows:

(1) *DC capacitance:* C_i = 1000 μF, C = 100 μF;
(2) *Filter inductance:* L = 200 μH;
(3) *Switching frequency:* f_s = 20 kHz.

To compare the performance of the proposed extension MPPT algorithm which can automatically adjust the step size with the conventional fixed step size P&O and INC MPPT methods, the simulations are configured under the same conditions. The sampling period used for the P&O and INC MPPT algorithm is chosen as 0.01 s. Therefore, the duty cycle of the power converter is updated every 0.01 s. The output power performance of P&O and INC MPPT methods with a fixed step size 0.01 under an insolation step change from 1000 W/m^2 (at temperature T = 45 °C) to 800 W/m^2 (at temperature T = 40 °C) at 0.3 s are shown in Fig. 7a and b, respectively. For the comparison, the corresponding PV output power response of the proposed extension MPPT method with allowable maximum duty size ΔD_{max} = 0.05 is also shown in Fig. 7c. It is obvious the oscillations occurring at steady-state in P&O and INC MPPT are almost eliminated by the extension MPPT algorithm. Also, the dynamic performance of the proposed method is obviously faster than the P&O and INC MPPT with fixed step size 0.01. To further verify the robustness of the proposed extension MPPT method, the simulated power responses due to solar insolation step change from 400 W/m^2 (at temperature T = 29 °C) to 500 W/m^2 (at temperature T = 35 °C) with the P&O, INC and extension MPPT methods are also shown in Fig. 8a–c for comparison. The results point out the oscillations at steady-state are greatly reduced by utilizing the proposed extension MPPT algorithm. Meanwhile, the dynamic response performance due to insolation change is improved, also.

5. Conclusions

An extension maximum power point tracking method was presented in this paper. This method combined the extension theory with a boost converter to speed up responses for reaching the accurate MPP of PV arrays under solar insolation and ambient temperature changes. In addition, the proposed extension MPPT method can also improve the steady-state performance and energy conversion efficiency. Both fixed step size MPPT methods (P&O and INC) and the proposed variable step size extension MPPT methods are established with the PSIM circuit-based model for simulation. The simulation results demonstrate the effectiveness and robustness of the proposed method. Further, the proposed intelligent MPPT algorithm needs less constructed data, and no learning procedure so it can be easily implemented using a microcontroller in the future.

Acknowledgement

The authors would like to thank the Photovoltaic Technology Center, Industrial Technology Research Institute, Taiwan for financially supporting this research.

References

Cai, W. (1983). The extension set and incompatibility problem. *Journal of Scientific Exploration, 1*, 81–93.
Chao, K. H., Ho, S. H., & Wang, M. H. (2008). Modeling and fault diagnosis of a photovoltaic system. *Electric Power Systems Research, 78*, 97–105.
Desai, H.P., & Patel, H.K. (2007). Maximum power point algorithm in PV generation an overview. In: *Proceedings of power electronics and drive systems*.
Esram, T., & Chapman, P. L. (2007). Comparison of photovoltaic array maximum power point tracking techniques. *IEEE Transactions on Energy Conversion, 22*, 439–449.
Femia, N., Granozio, D., Petrone, G., Spagnuolo, G., & Vitelli, M. (2007). Predictive & adaptive MPPT perturb and observe method. *IEEE Transactions on Aerospace Electronics Systems, 43*, 934–950.
Godoy Simoes, M., & Franceschetti, N. N. (1999). Fuzzy optimisation based control of a solar array system. *IEE Proceedings-Electric Power Application, 146*, 93–109.
Hart, D. W. (1997). *Introduction to power electronics*. New Jersey: Prentice Hall.
Khaehintung, N., & Sirisuk, P. (2007). Application of maximum power point tracker with self-organizing fuzzy logic controller for solar-powered traffic lights. In: *Proceedings of power electronics and drive systems*.
Kim, I., Kim, M., & Youn, M. (2006). New maximum power point tracker using sliding-mode observer for estimation of solar array current in the grid-connected photovoltaic system. *IEEE Transactions on Industrial Electronics, 53*, 1027–1035.
Kottas, T. L., Boutalis, Y. S., & Karlis, A. D. (2006). New maximum power point tracker for PV arrays using fuzzy controller in close cooperation with fuzzy cognitive networks. *IEEE Transactions on Energy Conversion, 21*, 793–803.
Koutroulis, E., Kalaitzakis, K., & Voulgaris, N. C. (2001). Development of a microcontroller-based, photovoltaic maximum power point tracking control system. *IEEE Transactions on Power Electronics, 16*, 46–54.
Liu, F., Duan, S., Liu, B., & Kang, Y. (2008). A variable step size INC MPPT method for PV systems. *IEEE Transactions on Industrial Electronics, 55*, 2622–2628.
Masoum, M. A. S., Dehbonei, H., & Fuchs, E. F. (2002). Theoretical and experimental analyses of photovoltaic systems with voltage-and current-based maximum power-point tracking. *IEEE Transactions on Energy Conversion, 17*, 514–522.
Powersim Inc. (2001–2003). PSIM User's Guide.
Sera, D., Kerekes, T., Teodorescu, R., & Blaabjerg, F. (2006). Improved MPPT method for rapidly changing environmental conditions. In: *Proceeding of IEEE ISIE*.
Siemens Solar Industries (1998). SIEMENS Solar module SP75 Specifications.
Veerachary, M., Senjyu, T., & Uezato, K. (2003). Neural-network-based maximum-power-point tracking of coupled-inductor interleaved-boost converter-supplied PV system using fuzzy controller. *IEEE Transactions on Industrial Electronics, 50*, 749–758.
Wu, L., Zhao, Z., & Liu, J. (2007). A single-stage three-phase grid-connected photovoltaic system with modified MPPT method and reactive power compensation. *IEEE Transactions on Energy Conversion, 22*, 881–886.
Wu, T. F., Chang, C. H., & Chen, Y. K. (2000). A fuzzy-logic-controlled single-stage converter for PV-powered lighting system applications. *IEEE Transactions on Industrial Electronics, 47*, 287–296.